Carbohydrate Polymers xxx (2012) xxx–xxx

Contents lists available at SciVerse ScienceDirect

Carbohydrate Polymers

journal homepage: www.elsevier.com/locate/carbpol

Cellular uptake and cytotoxicity of chitosan–caseinophosphopeptides nanocomplexes loaded with epigallocatechin gallate

Bing Hu[a,b], Yuwen Ting[a], Xiaoxiong Zeng[b,*], Qingrong Huang[a,**]

[a] Department of Food Science, Rutgers University, 65 Dudley Road, New Brunswick, NJ 08901, USA
[b] College of Food Science and Technology, Nanjing Agricultural University, Nanjing 210095, People's Republic of China

ARTICLE INFO

Article history:
Received 29 October 2011
Received in revised form 2 March 2012
Accepted 3 March 2012
Available online xxx

Keywords:
Chitosan–caseinophosphopeptides nanoparticles
Epigallocatechin gallate
Cellular toxicity
Cellular uptake
Intestinal absorption

ABSTRACT

Epigallocatechin gallate (EGCG) was successfully encapsulated in novel nanocomplexes assembled from bioactive peptides, caseinophosphopeptides (CPPs), and chitosan (CS), a natural cationic polymer. Their particle sizes and surface charges were determined to be in the range of 150.0 ± 4.3 nm and 32.2 ± 3.3 mV respectively. Crosslinking between the $-NH_3^+$ groups of CS with the $-P{=}O^-$ and $-COO^-$ groups of CPP, as well as the hydrogen bonding were confirmed from the FTIR results. Atomic force microscopy (AFM) images showed that EGCG loaded CS–CPP nanocomplexes were spherical in shape. Maintaining the surface charge as high as +32.2 mV, crosslinking CS with peptides reduced the cytotoxicity of CS nanoparticles. In addition, cellular internalization of EGCG-loaded CS–CPP nanoparticles was confirmed from green fluorescence inside the Caco-2 cells. The process of nanoparticle uptake was dose and time dependent in the range of time and concentration studied. Furthermore, the intestinal permeability of EGCG using Caco-2 monolayer was enhanced significantly as delivered by nanoparticles, which indicated the promising elevation of EGCG bioavailability.

1. Introduction

The health promotion properties of nutraceuticals, such as plant polyphenols and carotenoids, have attracted a lot of attention in recent years because their biological and pharmacological effects including antioxidative, anticancer, and chronic disease prevention properties have been demonstrated in numerous animal, human, and in vitro studies (Frei & Higdon, 2003b; Khan, Afaq, Saleem, Ahmad, & Mukhtar, 2006; Lambert, Hong, Yang, Liao, & Yang, 2005; Sang et al., 2005). However, the major challenge of dietary nutraceuticals is their poor oral bioavailability, and one key barrier to the absorption of nutraceuticals is intestinal epithelium because it is difficult for many nutraceuticals to diffuse across the cells through the lipid-bilayer cell membranes (Manach, Scalbert, Morand, Remesy, & Jimenez, 2004; van Duynhoven et al., 2011). In order to realize the full potential of these agents, there is a need to improve their intestinal absorption. One strategy, which has been proved effective for poorly absorbed drugs, is the use of colloidal nanoparticle delivery systems prepared from nontoxic and biodegradable materials (Kohane, Timko, & Dvir, 2010; Minko, Motornov, Roiter, & Tokarev, 2010). The possible mechanisms include increasing the apparent solubility of the active ingredient, increasing the rate of mass transfer, increasing the retention time or increasing the absorption via direct uptake of the nanoparticle carriers (Acosta, 2009).

In the field of food nanotechnology, nanoparticle delivery systems for nutrients and nutraceuticals with poor water solubility but high intestinal permeability have been expanded to increase their solubility (Kaur, Kakkar, Singh, & Singla, 2011; McClements & Rao, 2011). Until now, most of the researches on nanoparticle vehicles are concentrated on developing production methods inspired by pharmaceutical drug delivery systems, such as emulsion and micelle (Sagalowicz & Leser, 2010). However, rare studies have been carried out focusing on design of nanoparticle delivery system for the soluble but poorly absorbed ingredients such as EGCG (Acosta, 2009; Lvov et al., 2009; Mukhtar et al., 2009). EGCG, the most abundant and active catechin in green tea, has been shown to inhibit the formation and development of tumors in different organs in animal models. It is a well-studied chemopreventive agent, and has shown remarkable chemopreventive potential (Amin, Kucuk, Khuri, & Shin, 2009; Tammela et al., 2004). EGCG can inhibit enzyme activities and signal transduction pathways, resulting in the suppression of cell proliferation and enhancement of apoptosis, as well as the inhibition of cell invasion, angiogenesis and metastasis (Yang, Wang, Lu, & Picinich, 2009). However, the concentrations that appear effective in blocking tumor cell proliferation or inducing apoptosis in vitro are often an order of magnitude higher than levels measured in vivo. EGCG

* Corresponding author. Tel.: +86 25 84396791.
** Corresponding author. Tel.: +1 732 932 7193.
E-mail addresses: zengxx@njau.edu.cn (X. Zeng), qhuang@aesop.rutgers.edu (Q. Huang).

0144-8617/$ – see front matter © 2012 Elsevier Ltd. All rights reserved.
doi:10.1016/j.carbpol.2012.03.015

has quite low bioavailability in oral consumption, which was confirmed due to their poor small intestinal absorption rather than hepatic elimination (Cai, Anavy, & Chow, 2002). As a consequence, relatively small amount of EGCG can enter blood stream, further reach the target site. Therefore, design of nanoparticles that are suitable for oral consumption and able to enhance the small intestinal absorption of EGCG is very important. In our previous study, novel nanoparticles have been successfully assembled from CS and CPPs (Hu, Wang, Li, Zeng, & Huang, 2011), and such delivery systems have the potential of improving the bioavailability of active ingredients, especially for compounds such as EGCG that is soluble in water but having low permeability in small intestine.

Direct nanoparticle uptake was expected to play an essential role in improving the intestinal absorption of the soluble but poorly absorbed ingredients (Acosta, 2009). To date, the internalization of nanoparticles into the cells was achieved through cellular pinocytosis (Schmid & Conner, 2003). Recently, several reports have discussed the pinocytosis of CS nanoparticles into cells by basic mechanisms such as clathrin-mediated endocytosis (CME), caveolae-mediated endocytosis, macropinocytosis and lipid raft-mediated endocytosis (Chiu et al., 2010; Nam et al., 2009). Among these mechanisms, caveolae-mediated endocytosis and lipid raft-mediated endocytosis have been confirmed to be the dominant ones. After entering cells, the CS nanoparticles were firstly intracellular trafficked to endosomes, and finally were entrapped in lysosomes (Chiu et al., 2010).

The human colon carcinoma cell line Caco-2 cells grown on permeable filters have become the golden standard for in vitro prediction of intestinal drug permeation and absorption (Artursson, Hubatsch, & Ragnarsson, 2007). In culture, this cell line slowly differentiates into monolayers with a differentiated phenotype with many functions of the small intestinal villus epithelium. The in vivo absorption is mainly predicted from the apparent permeation rate (P_{app}) across the Caco-2 cell monolayers. Although the P_{app} obtained from different laboratories are different, there is a general trend that a high P_{app} implies a high absorption. According to previous reports, the P_{app} values for catechins including EGCG ranged from 0.8 to 3.5×10^{-7} cm/s (Sugihara, Kadowaki, Tagashira, Terao, & Furuno, 2008; Zhang, Zheng, Chow, & Zuo, 2004), which are exceptionally low (Teitelbaum, Yang, & Finaly, 2003).

In present study, CS–CPP nanoparticles were utilized to encapsulate EGCG as its delivery system. The interaction between CS and CPP was confirmed from the FTIR analysis and compared with the interaction between CS and tripolyphosphte (TPP). CS–CPP nanoparticles loaded with EGCG were characterized by atomic force microscopy (AFM), dynamic light scattering (DLS) and electrophoretic mobility (zeta potential). Although composed of both food-grade polymers, the cytotoxicity of the nanoparticles is still a concern in developing EGCG delivery systems. The cytotoxicity of CS–CPP nanoparticles was determined by MTT assay using Caco-2 cells. In addition, the cellular uptake fate of the fluorescently labeled CS–CPP nanoparticles analogs was investigated via fluorescence microscopy. Furthermore, intestinal permeability or absorptivity of free and nanoencapsulated EGCG were predicted based on Caco-2 cell monolayer model.

2. Materials and methods

2.1. Materials

CPPs were prepared and identified with HPLC–MS–MS as described in our previous study (Hu, Wang, Li, Zeng, & Huang, 2011). CS of the molecular weights 100 kDa, derived from crab shell, was obtained from Golden-Shell Biochemical Co. Ltd. (Hangzhou, China). The degree of deacetylation was 90%. EGCG, 2′,7′-dichlorofluorescin diacetate (DCFH-DA), ethanol were purchased from Sigma–Aldrich, Inc. (St. Louis, MO). Dimethyl sulfoxide, HPLC grade of acetonitrile (MeCN) and acetic acid were obtained from Fisher Scientific (Pittsburgh, PA). Caco-2 cell line was generously provided by Dr. Judith Storch, Department of Nutrition, Rutgers, the State University of New Jersey, USA. Sodium carbonate, acetone, and methanol were obtained from Mallinckrodt Baker, Inc. (Phillipsburg, NJ). Williams' Medium E (WME), Hanks' Balanced Salt Solution (HBSS) and MEM/EBSS were purchased from HyClone Laboratories, Inc. (Logan, Utah). Fetal bovine serum (FBS) was obtained from Atlanta Biologicals (Lawrenceville, GA). Other chemicals were of reagent grade and used without further purification.

2.2. General procedure for preparation of nanoparticles

CS–CPP nanoparticles were prepared according to our procedure reported previously (Hu, Wang, Li, Zeng, & Huang, 2011). Briefly, CS was dissolved in 1% (w/v) acetic acid solution with sonication until the solution was transparent. The aqueous solution of CPP was obtained at a suitable concentration. Both CS and CPP solutions were adjusted to pH 6 with 1 N HCl or NaOH solution. Subsequently, CS solution was added to CPP solution under stirring at room temperature. The formation of CS–CPP nanoparticles started spontaneously via the CPP initiated ionic gelation mechanism. For the preparation of EGCG loaded CS–CPP nanoparticles, the aqueous solution of EGCG was added into CPP solution before the addition of CS solution. CS–TPP nanoparticles were prepared according to our previous study (Hu et al., 2008) with the same concentration of CS as that in CS–CPP nanoparticles. The nanoparticle suspensions were immediately subjected to further analysis and applications.

2.3. Characterization of nanoparticles

The mean particle size and size distribution were determined using dynamic light scattering (DLS)-based BIC 90 plus particle size analyzer equipped with a Brookhaven BI-9000AT digital correlator (Brookhaven Instrument Corporation, New York, NY, USA) at a fixed scattering angle of 90° at 25 ± 1 °C. All these measurements were made in triplicate at 25 ± 1 °C.

Electrophoretic mobility (UE) (a particle's velocity in an electric field) for homogenous and mixed CS–CPP systems was investigated using a Zetasizer Nano-ZS90 (Malvern Instruments, Westborough, MA, USA). All measurements were made in triplicate.

Morphological evaluation of the nanoparticles was performed by AFM. Sample solution was dip-coated on a freshly cleaned mica for 1 h and dried by nitrogen. All AFM images were recorded with a Digital Instruments Nanoscope IIIa Multimode in tapping mode at room temperature using a silicon tip with nominal spring constant of 40 N/m.

The FTIR spectral were collected under ambient conditions, using a Thermal Nicolet Nexus 670 FTIR spectrometer (Thermo Electron Corp., Madison, WI) equipped with a Smart MIRacle horizontal attenuated total reflectance Ge crystal accessory. Each spectrum was averaged over 256 scans with 4 cm^{-1} resolution in the range of 500–4000 cm^{-1}.

2.4. In vitro cytotoxicity of CS–CPP nanoparticles on Caco-2 cells

Caco-2 cells were seeded onto 96-well plates at a density of 50,000 cells/well and cultured in 200 μL of Dulbecco's Modified Eagle Medium for 24 h in the CO_2 incubator. The spent medium was replaced with CS–CPP nanoparticles and diluted with culture medium to give a CS concentration from 0.5–0.002 mg/mL (pH 6.2). After overnight incubation at 37 °C, the CS–CPP nanoparticles were replaced with 100 μL of MTT (0.5 mg/mL in PBS, pH 7.4) solutions, and the cells incubated for a further 2.5 h at 37 °C. The test

Please cite this article in press as: Hu, B., et al. Cellular uptake and cytotoxicity of chitosan–caseinophosphopeptides nanocomplexes loaded with epigallocatechin gallate. *Carbohydrate Polymers* (2012), doi:10.1016/j.carbpol.2012.03.015

solution was decanted, and 100 μL of DMSO (MTT assay) was added to solubilize the cells. The resultant solutions were measured in a microplate reader (Molecular Devices Corporation, Palo Alto, CA, USA) at λ = 570 nm. Cell viability was expressed as percentage of absorbance relative to control, the control cells not exposed to the CS materials. Experiments were performed in triplicate, with six replicate wells for each sample and control per assay.

2.5. Cellular uptake of nanoparticles

Fluorescein isothiocyanate (FITC) labeled CS (FCS) was synthesized by adding 50 mL of dehydrated methanol followed by 25 mL of FITC in methanol (2.0 mg/mL) to 50 mL of CS (1% in 0.1 M HAc) in the dark at ambient temperature. After 3 h, the labeled polymer was precipitated in 0.25 M NaOH. The precipitate was pelleted at 4000 × *g* (10 min) and washed with methanol:water (70:30, v/v). The washing and pelletization were repeated until no fluorescence was detected in the supernatant (Cary Eclipse Fluorescence Spectrophotometer, Varian Instruments, Walnut Creek, CA, λ_{exc} = 492 nm, λ_{emi} = 520 nm). The labeled CS was re-dissolved in 25 mL of 0.1 M acetic acid (HAc) and dialyzed in the dark against 5 L of water for 3 days, the water being replaced with fresh water every 6 h. Finally, the labeled CS was freeze-dried.

FITC-labeled CS–CPP nanoparticles containing EGCG (FNPE) were prepared as described in Section 2.2 by replacing CS with FITC-labeled CS (FCS). Caco-2 cells between passages 8 and 20 were seeded onto Lab-Tek® Chambered Coverglasses (Thermo Scientific Nunc®, Thermo Scientific) at a density of 5×10^4 cells/cm^2 and cultured in 0.6 mL of MEM growth medium at 37 °C in the incubator. After 2 days of culture, the cell monolayers were washed twice and pre-incubated with 0.6 mL of pre-warmed transport medium (pH 6.2) for 30 min at 37 °C. Uptake was initiated by adding 0.6 mL of FNPE or FCS solution diluted by the medium to final chitosan concentration of 0.125 mg/mL. After 2 h of incubation at 37 °C, the FNPE or FCS was removed, and the cells were washed twice with pre-warmed PBS solution, fixed in 4% paraformaldehyde for 10 min. The specimens after storage overnight at 4 °C in Cell Freezing Medium-Serum-free (Sigma, USA) were examined under a fluorescence microscope. The fluorescence micrographs were recorded with a Nikon TE-2000-U inverted fluorescence microscope equipped with a CCD camera (Retiga EXi, QImaging). Images were taken at the same region under visible light and bandpass filter to observe the fluorescence signals emitting from FNPE or FCS (excitation: 488 ± 10 nm and emission: 520 ± 10 nm). All images were processed by C-Imaging software (SimplePCI, Compix Inc.).

2.6. Transport of EGCG through Caco-2 cell monolayer

Caco-2 cells were maintained in DMEM with 10% FBS, 1× nonessential amino acids and 1× penicillin and streptomycin, at 37 °C with 5% CO_2. Cells of passage 37–45 were used in this study, to keep relatively constant cellular phenotypes.

Procedures for determination of the apparent permeation rate (P_{app}) of EGCG encapsulated in CS–CPP nanoparticles across Caco-2 generally followed the detailed protocol reported previously (Artursson, Hubatsch, & Ragnarsson, 2007). To generate Caco-2 cell monolayers in the insert filters of 12-well plates, 0.5 mL Caco-2 cells were plated onto the insert (the apical compartment) at the density of 6×10^5 cell/mL. One and a half mL culture media were subsequently added in the lower (basolateral) compartment of each well. Media were changed every two days. Permeation experiments were performed after 29–31 days of plating. In the permeation experiments, HBSS + 10 mM hydrochloric acid, pH 6.2 is used as transport solution. EGCG at constant concentration (50 μM) was encapsulated by various CS–CPP nanoparticle concentrations at 0.0625 mg/mL, 0.125 mg/mL and 0.25 mg/mL as donor media. In the permeation direction of apical to basolateral (A–B) compartment, 0.4 mL donor media was added to the apical compartment and 1.2 mL receiving media (same as transport solution) were added to the basolateral compartment. Plates were then put in a shaker at 100 rpm at 37 °C. At 30, 60, 90, and 120 min of permeation, half volumes of the receiving media were removed and the same volumes of fresh media were replenished. The removed receiving media were diluted to 1 mL by HPLC grade water and then analyzed with HPLC for EGCG quantification according to our previous method (Hu et al., 2009). Cumulative quantity of EGCG permeated at each time interval was calculated and plotted against time. The initial slope was then used to calculate the P_{app} using the following equation:

$$P_{app} = \left(\frac{dQ}{dt}\right)\left(\frac{1}{AC_0}\right) \quad (1)$$

where dQ/dt is the rate of EGCG permeation. A is the surface area of the insert (1.1 cm^2), C_0 is the EGCG concentration.

To ensure the integrity of Caco-2 monolayers, transepithelial electrical resistance (TEER) value is determined. TEER value was measured before each experiment using Evohm2 epithelial voltmeter (World Precision Instruments), and calculated as

$$\text{TEER}\ (\Omega\,\text{cm}^2) = (\text{TEER}\,(\Omega) - \text{TEER}_{\text{background}}\ (\Omega)) \times \text{Area}(\text{cm}^2) \quad (2)$$

where TEER (Ω) is the electrical resistance across Caco-2 monolayers directly read from the Evohm2 epithelial voltmeter, $\text{TEER}_{\text{background}}$ (Ω) is that across the insert only (without cells). Area (cm^2) is the area of the insert, 1.1 cm^2.

3. Results and discussion

3.1. Preparation of EGCG loaded CS–CPP nanoparticles

In our previous study, CS–CPP nanoparticles have already been prepared through the electrostatic and hydrophobic interactions between CS and CPP (Hu, Wang, Li, Zeng, & Huang, 2011). Here, EGCG was encapsulated into the nanoparticles through introducing aqueous solution of EGCG into CPP solution before the addition of CS solution. It is well known that polyphenols can associate with proteins to form soluble and insoluble complexes (Barrand, Cooray, Janvilisri, van Veen, & Hladky, 2004; Panda, Manna, Mukherjee, Roy, & Das, 2009). The same phenomenon appeared in our study when EGCG was added into peptide solution, indicated from the slightly increased turbidity of the mixture solution. Compared with trapping tea catechin in CS–TPP nanoparticles (Hu et al., 2008), the interaction between EGCG and CPP provided direct drive for encapsulation of EGCG in the CS–CPP nanoparticles. As the physicochemical features of CS nanoparticles loaded with target molecules may affect the stability as a result of stable ionic interactions and biological performance, it is important to elucidate the effect of preparation conditions on characteristics of CS nanoparticles loaded with target molecules. Therefore, we investigated the effects of CS/CPP mass ratio (fixed EGCG concentration), EGCG/CPP mass ratio (fixed CS concentration) on surface morphology, particle size, polydispersity indexes (PDI), and surface charge of EGCG loaded CS–CPP nanoparticles.

Fig. 1A shows the change of particle size and surface charge of the EGCG loaded CS–CPP nanoparticles with the increase of CS/CPP mass ratio at a fixed concentration of EGCG. Similar to the change trends in our previous study (Hu, Wang, Li, Zeng, & Huang, 2011), the increase of CS/CPP mass ratio caused the particle size to sharply decrease from about 930 nm to a steady state at around 150 nm. The final particle size is bigger than the CS–CPP nanoparticles without EGCG (115 nm), which is caused by the encapsulation of EGCG. The polydispersity indexes (PDIs) of the nanoparticle suspensions ranged from 0.05 to 0.14, indicating that a homogeneous dispersion

Please cite this article in press as: Hu, B., et al. Cellular uptake and cytotoxicity of chitosan–caseinophosphopeptides nanocomplexes loaded with epigallocatechin gallate. *Carbohydrate Polymers* (2012), doi:10.1016/j.carbpol.2012.03.015

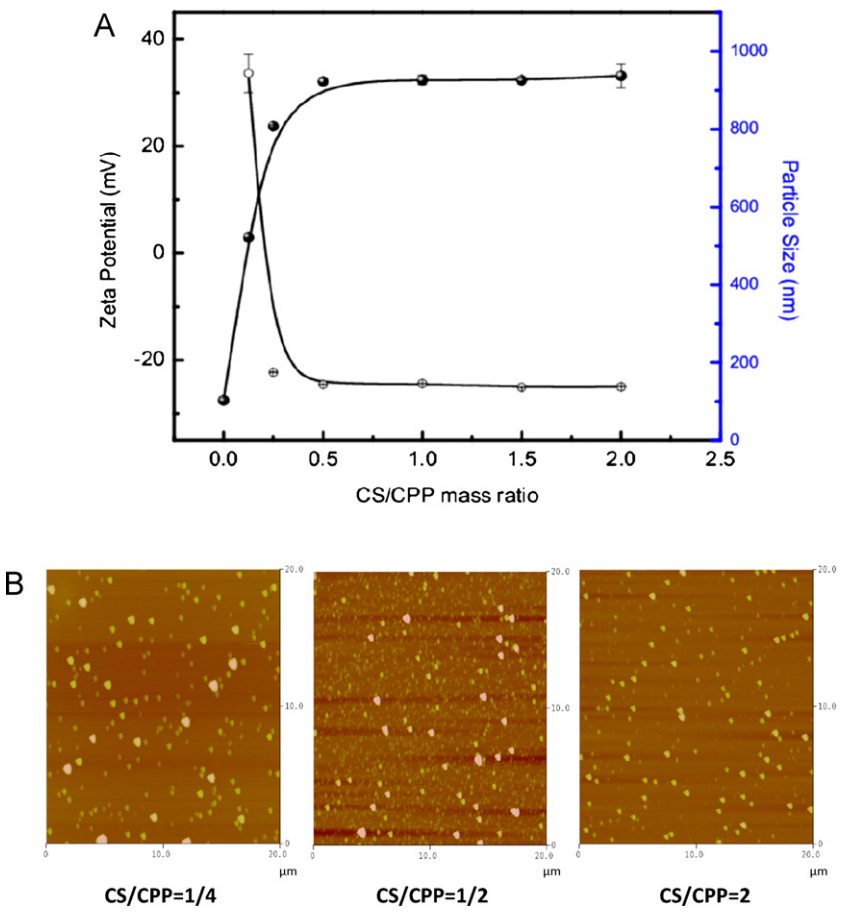

Fig. 1. (A) Effect of chitosan/caseinophosphopeptides mass ratio on particle size (○) and zeta potential (●) of EGCG loaded chitosan–caseinophosphopeptides nanoparticles. (B) AFM images of the nanosuspensions with different chitosan/caseinophospho-peptides mass ratios. The concentrations of caseinophosphopeptides and EGCG were fixed at 1 mg/mL and 0.6 mg/mL respectively, and the pH was fixed at 6.2.

of nanoparticles was obtained. Meanwhile, the surface charge of the nanoparticles (Zeta potential) increased sharply from negative to positive, then reached a plateau with gradual increase to around +32.2 mV. Generally, a zeta potential of at least +30 mV is required for a physically stable nanosuspension solely stabilized by electrostatic repulsion. Fig. 1B shows the surface AFM morphology of the EGCG loaded CS–CPP nanoparticles at different CS/CPP mass ratios of 1/4, 1/2 and 2 with the scan size of 20 μm. CS–CPP nanoparticles were regularly spherical in shape and dispersed homogenously. In Fig. 1A, the particle size decreased slightly with the increase of CS/CPP mass ratios from 1/4 to 1/2, then to 2. With the same change trend, it can be seen from the AFM images in Fig. 1B that the particle size also decreased as the CS/CPP mass ratios increased from 1/4 to 2. Therefore, the changes of nanoparticles morphology shown in AFM images are in consistent with the change of particle sizes determined by DLS.

It can be seen from Fig. 2A that the particle sizes increased from 128.2 to 157.7 nm with the increase of the EGCG/CPP mass ratio at the fixed CS concentration. With the increase of EGCG/CPP mass ratio, surface charge of the nanoparticles loaded with EGCG firstly decreased from 30.0 to 26.8 mV. Further increase of EGCG/CPP mass ratio caused zeta potential to increase again to 32.2 mV. This phenomenon might be caused by the interaction between EGCG and CPP, which further influenced the cross-linking degree between CPP and CS. The EGCG loaded nanoparticles were generated by the electrostatic interaction between anionic CPP and cationic CS (Hu, Wang, Li, Zeng, & Huang, 2011). In addition, CPP could interact with EGCG through hydrophobic association and the specific interaction between the A and D (gallate group) rings of EGCG with proline in CPP (Hu et al., 2012). Phenolic groups of EGCG can be deprotonated at pH 6.2 and the generated oxygen center could impart a high negative charge density. Under low EGCG/CPP mass ratios, EGCG absorbed to CPP molecules, which could enhance the electrostatic neutralization of CS with CPP, resulting in a decrease of surface charge. However, with further increase of EGCG/CPP mass ratios, CPP were highly cross-linked by EGCG through the formation of nanocomplexes, which could weaken the electrostatic neutralization of CS with CPP to certain extent, resulting in an increase of surface charge. The corresponding surface AFM morphology of EGCG loaded CS–CPP nanoparticle at different EGCG/CPP mass ratio is shown in Fig. 2B (in the scan scale of 20 μm). It can be seen that, with the increase of EGCG/CPP mass ratios from 0.1 to 0.4, then to 0.7, the particle sizes increased and more aggregates of the nanoparticles appeared, resulting in the increase of particle sizes as determined by DLS.

3.2. FTIR

The crosslinking interactions between CS and CPP were confirmed through FTIR measurements (Fig. 3). The characteristic peaks of CS appeared at 3400, 3300, 1560, and 1080 cm^{-1}, corresponding to its hydroxyl (OH), amine (NH_2), amide II (N—H bending vibrations coupled to C—N stretching vibrations) groups, and glycosidic linkage (C—O—C), respectively (Huo, Zhang, Zhou, Yu, & Wu, 2009). The characteristic peaks of CPP appeared at 3300, 1631 and 1150 cm^{-1}, corresponding to its N—H bending, carboxylic acid group (—COOH) vibrations and —P=O$^-$ bending respectively (Sung et al., 2008). Compared with neat CS and neat CPP, the peaks around

Please cite this article in press as: Hu, B., et al. Cellular uptake and cytotoxicity of chitosan–caseinophosphopeptides nanocomplexes loaded with epigallocatechin gallate. *Carbohydrate Polymers* (2012), doi:10.1016/j.carbpol.2012.03.015

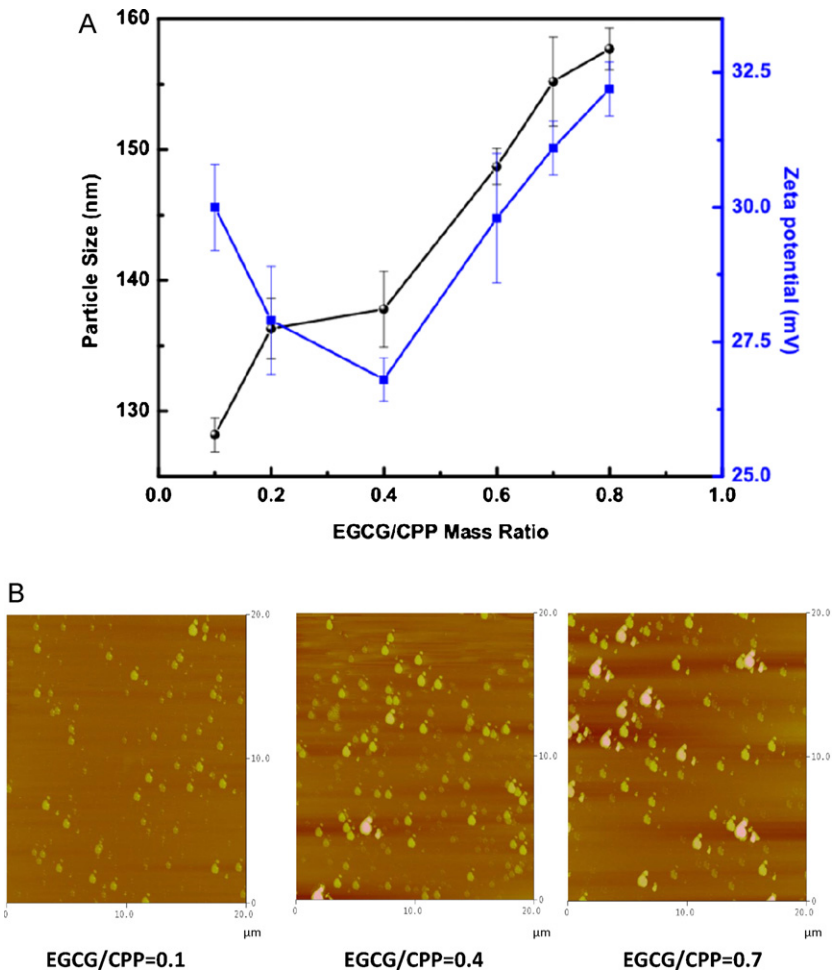

Fig. 2. (A) Effect of EGCG/caseinophosphopeptides mass ratio on particle size (●) and zeta potential (■) of EGCG loaded chitosan–caseinophosphopeptides nanoparticles. (B) AFM images of the nano-suspension with different EGCG/caseinophosphopeptides mass ratio. The concentrations of both chitosan and caseinophosphopeptides were 1 mg/mL, and the pH was fixed at 6.2.

3400–3300 cm^{-1} in CS–CPP nanoparticles disappeared, indicating the enhanced hydrogen bonding between —OH in CS with —COO^- and PO^{3-} in CPP (Fu, Wu, Yang, Wang, & Hu, 2005). In addition, compared with neat CPP, in spectrum of CS–CPP nanoparticles, the absorption peaks of 1631 cm^{-1} (carboxyl group absorption peak) and 1150 cm^{-1} (—P=O^- group absorption peak) disappeared. Furthermore, a peak, at 1407 cm^{-1}, arose in both of the CS–CPP and CS–TPP nanoparticles, but was not observed for neat chitosan or neat CPP. We attribute this peak to the —NH^{3+} groups of chitosan ionic cross-linked with the —P=O^- as well as —COO^- groups of CPP and the —P=O^- group of TPP (Tsao et al., 2010).

3.3. Cytotoxicity of CS–CPP nanoparticles

The determination of cell viability is a common assay to evaluate the in vitro cytotoxicity of biomaterials. In the present study, cell viability was assessed by the MTT assay, which is a quantitative and rapid colorimetric method based on the cleavage of a yellow tetrazolium salt (MTT) to insoluble purple formazan crystals by the mitochondrial dehydrogenase of viable cells. The cytotoxicity of CS as condensed CS–CPP nanoparticles was evaluated as a function of concentration. CS–CPP nanoparticles showed on cytotoxicity in the CS concentration range of 0.002–0.5 mg/mL as measured by the MTT assay (Fig. 4). Previous studies reported that CS nanoparticles had cytotoxicity in relatively high concentration of CS, which was directly proportional to the positive surface charge (zeta potential) (Huang, Khor, & Lim, 2004). On the other hand, surface charge is an important determinant in the stability, mucoadhesiveness, and permeation enhancing effect of the nanoparticles (Gaserod, Jolliffe, Hampson, Dettmar, & Skjak-Braek, 1998; Wood, Smith, & Dornish, 2004). Positively charged CS nanoparticles can interact through electrostatic interaction with the negatively charged mucin layer that coats the surface of enterocytes and M layers (Sung et al., 2008). In present study, although the surface charge was maintained at as high as +32.2 mV, cross-linking CS with peptides reduced the cytotoxicity of CS nanoparticles. It was reported that modification of polymer with peptides can elicit a specific cellular response, increasing the biocompatibility of biomaterials (Shoichet, 2010). This might be the reason for the significant reduction of cytotoxicity of CS–CPP nanoparticles.

3.4. Cellular uptake of nanoparticles

Firstly, the uptake efficiency of FNPE was compared with that of their precursor, the free form linear CS polymers of 100 kDa. Compared to the relatively robust FNPE nanoparticles, the CS polymer of a similar molecular weight may differ in shape and overall size as represented by the hydrodynamic volume in the media.

In order to visualize the uptake, CS was fluorescently labeled by treating with 0.2% of FITC in methanol. Here, the Caco-2 cells without any exposure to drug were used as control. Thus, three Caco-2 cell cultures, each containing FNPE, FCS, or only transport

Please cite this article in press as: Hu, B., et al. Cellular uptake and cytotoxicity of chitosan–caseinophosphopeptides nanocomplexes loaded with epigallocatechin gallate. *Carbohydrate Polymers* (2012), doi:10.1016/j.carbpol.2012.03.015

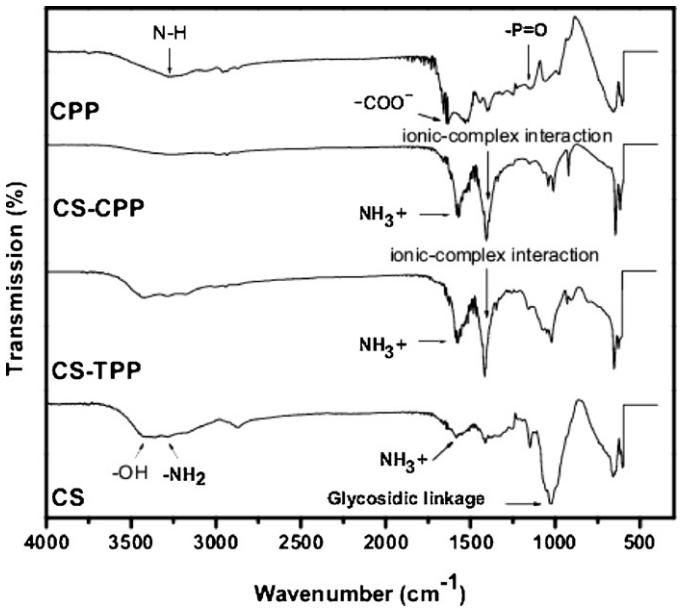

Fig. 3. FTIR spectra of chitosan, chitosan– tripolyphosphte nanoparticles, chitosan–caseinophosphopeptides nanoparticles and caseinophosphopeptides.

medium, were incubated (3 h, 37 °C). As their subcellular localization was tracked under a fluorescence microscope (Fig. 5), FNPE and FCS were clearly observed inside the cells as green color. Furthermore, cells treated with CS–CPP nanoparticles exhibited an intense fluorescence signal along the cell membrane and inside the cytosol, suggesting a strong uptake of CS–CPP nanoparticles. However, the control cells incubated only with transport medium did not show any fluorescence. It suggests that the physicochemical properties of CS–CPP nanoparticles may facilitate their adhesion to the cell membrane and the subsequent uptake. The irregular shape and random structure of CS may deter its entry into the cell (Nam et al., 2009).

Next, we monitored the internalization process of CS–CPP nanoparticles with respect to the treatment time and dose (Fig. 6). At the same condition in Fig. 5, FNPE (125 μg/mL) were added to the cultured Caco-2 cells and incubated at 37 °C with different incubation time of 0, 30, 60, 120 and 180 min. At the beginning of incubation (0 min), no fluorescence signal could be detected from Caco-2 cell incubated with FNPE (Fig. 6A). Then, with the increase of incubation time, it can be seen from the images that fluorescence intensity strengthened, which indicated that more and more CS–CPP nanoparticles could entry Caco-2 cells progressively. Fig. 6B displays the microscopic images of Caco-2 cells incubated with different concentrations of FNPE ranging from 0, 62.5, 125, 250 to 500 μg/mL with the fixed incubation time of 180 min. All the images of the cells incubated with different concentrations of FNPE (the same incubation time) showed green fluorescence. And the fluorescence intensity increased with the FNPE concentration. Therefore, the degree of nanoparticle uptake was clearly dose and time dependent in the studied concentration range.

3.5. Transport of EGCG through Caco-2 cell monolayer

Consumption of tea (*Camellia sinensis*) has been suggested to reduce the risk of cancer, cardiovascular disease and other diseases. These beneficial effects are attributed mainly to the presence of polyphenols in tea. EGCG, known as a strong natural antioxidant micronutrients in our diet, is the most abundant and active catechin in green tea (Frei & Higdon, 2003a). Previous researches with human cancer cell lines have demonstrated that EGCG is able to prevent cancer through inhibiting cyclin-dependent kinases, growth factor-related cell signaling, mitogen-activated protein kinases, activation of activator protein 1 (AP-1) and nuclear factor κB (NFκB), matrix metalloproteinases and topoisomerase I as well as other potential targets (Yang, Maliakal, & Meng, 2002). Although some studies report effects of EGCG at submicromolar levels, most experiments require concentrations of more than 10 or 20 μmol/L to demonstrate the effect. However, the peak plasma concentration of EGCG in humans is around 1 μmol/L mainly because tea EGCG undergoes glucuronidation, sulfation, methylation, efflux and ring fiss ion in intestine (Lambert & Yang, 2003). Therefore, increasing the bioavailability of EGCG is essential for realizing the full potential of EGCG as an effective functional compound.

Fig. 7 shows the cumulative amount of EGCG transported through Caco-2 cell monolayers incubated with free-formed EGCG solution, or nano-encapsulated EGCG with different nanoparticle concentrations as a function of time at pH 6.2, to mimic the acidic microenvironment in the small intestine. As shown, the amount of EGCG transported through Caco-2 cell monolayers from apical to basolateral side increased progressively with

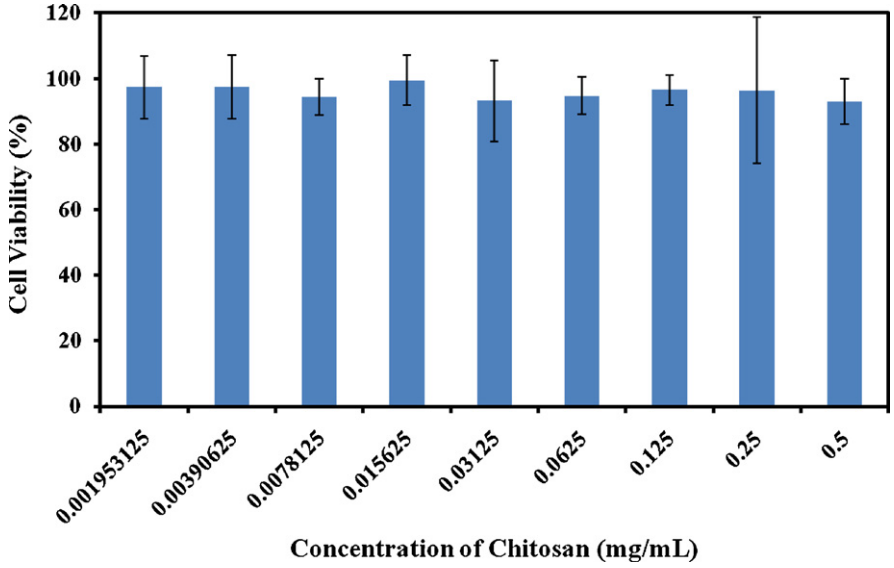

Fig. 4. In vitro cytotoxicity of chitosan–caseinophosphopeptides nanoparticles on cells as measured by the MTT assay. Cell viability was expressed as mean ± S.D ($n = 3$).

Please cite this article in press as: Hu, B., et al. Cellular uptake and cytotoxicity of chitosan–caseinophosphopeptides nanocomplexes loaded with epigallocatechin gallate. *Carbohydrate Polymers* (2012), doi:10.1016/j.carbpol.2012.03.015

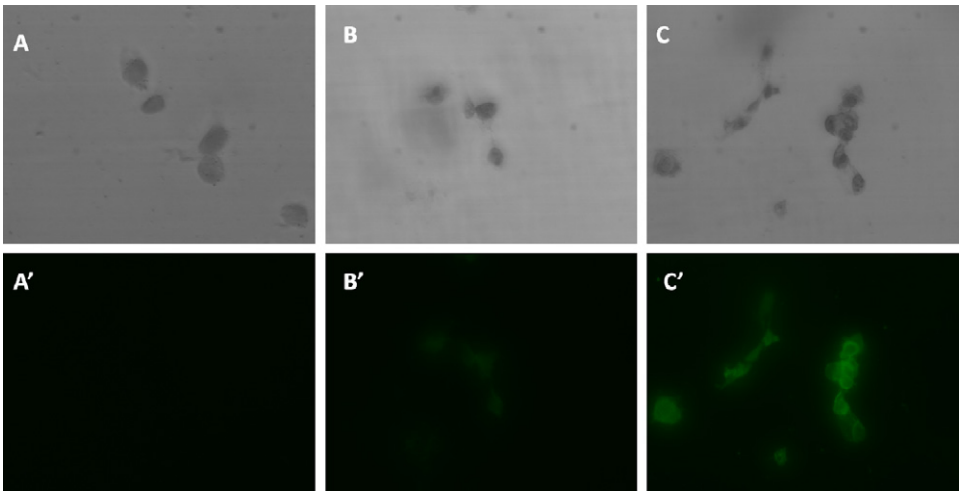

Fig. 5. Images of Caco-2 cells incubated with transport medium (A–A′), FITC-labeled chitosan (B–B′) and FITC-labeled chitosan–caseinophosphopeptides nanoparticles loaded with EGCG (C—C′) as visualized using inverted fluorescence microscope.

incubation time except the free one that no additional EGCG could be determined after 90 min. Compared with free one, encapsulation of EGCG with CS–CPP nanoparticles enhanced its transported amount progressively in accordance with the elevation of nanoparticle concentration. Furthermore, after encapsulated in the CS–CPP nanoparticles, the P_{app} of EGCG increased significantly with the maximum P_{app} values changing from 3.50×10^{-7} cm/s to 1.34×10^{-6} cm/s according to the increase of nanoparticle vehicle concentrations. The TEER values for all the Caco-2 cell monolayers before each experiment were in the range of 700–900 Ω cm^2. The TEER values of the cell monolayers incubated with nanoparticles decreased to the range of 250–400 Ω cm^2 after the experiments.

The enhanced permeation of EGCG after encapsulation with CS–CPP nanoparticles can be understood from cellular uptake of nanoparticles. Cellular uptake of CS–CPP nanoparticles loading with EGCG by Caco-2 cells have been confirmed in present study. After entering cells, the CS nanoparticles were firstly intracellular trafficked to endosomes, and finally were entrapped in lysosomes (Chiu et al., 2010). In these processes, CS nanoparticles were able to protect the encapsulated EGCG from being metabolized by blocking the contact between EGCG and corresponding glycosylase and methylase. Finally, EGCG was released as the CS nanoparticles were digested in lysosome. The acidic condition within lysosome around pH 4.5 was helpful for maintaining the stability of EGCG.

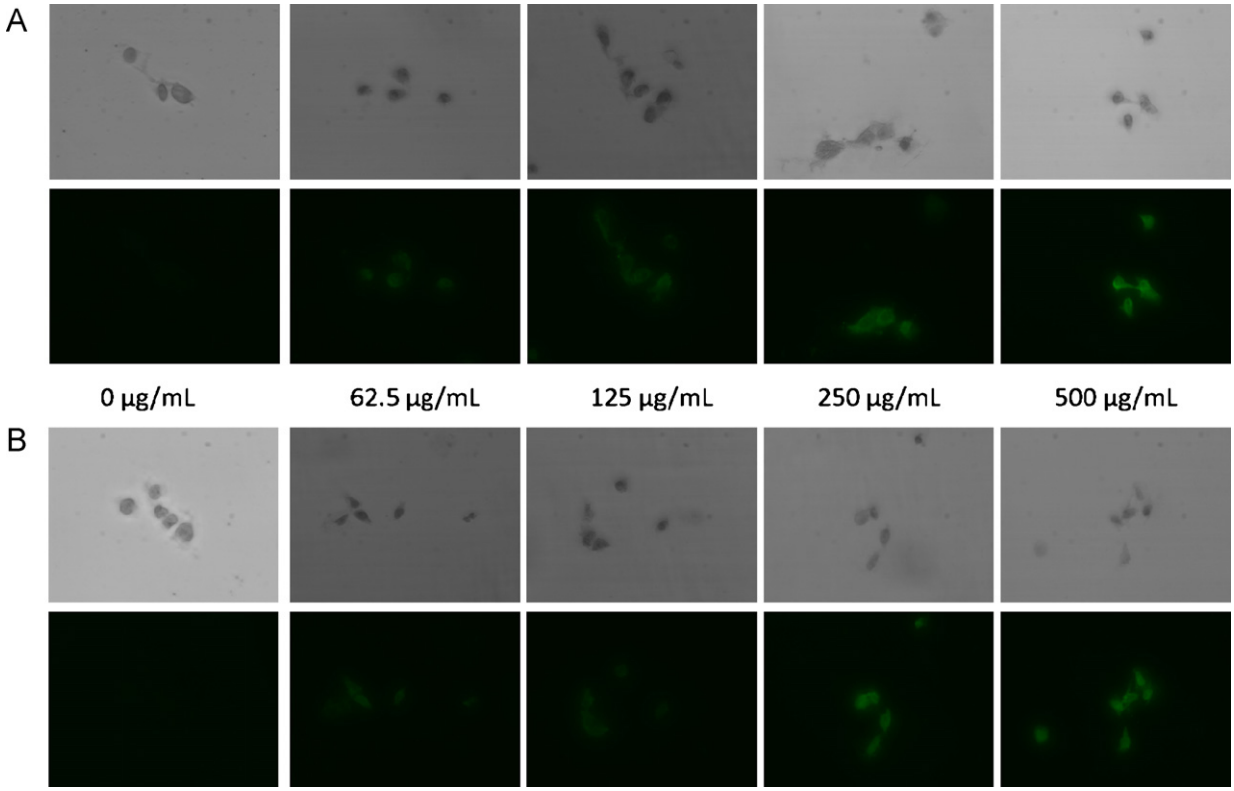

Fig. 6. Cellular uptake profile of chitosan–caseinophosphopeptides nanoparticles as a function of (A) incubation time (125 μg/mL, 37 °C) and (B) treatment concentration (3 h, 37 °C). Caco-2 cells were incubated with CS–CPP nanoparticles under the condition indicated in each image.

Please cite this article in press as: Hu, B., et al. Cellular uptake and cytotoxicity of chitosan–caseinophosphopeptides nanocomplexes loaded with epigallocatechin gallate. *Carbohydrate Polymers* (2012), doi:10.1016/j.carbpol.2012.03.015

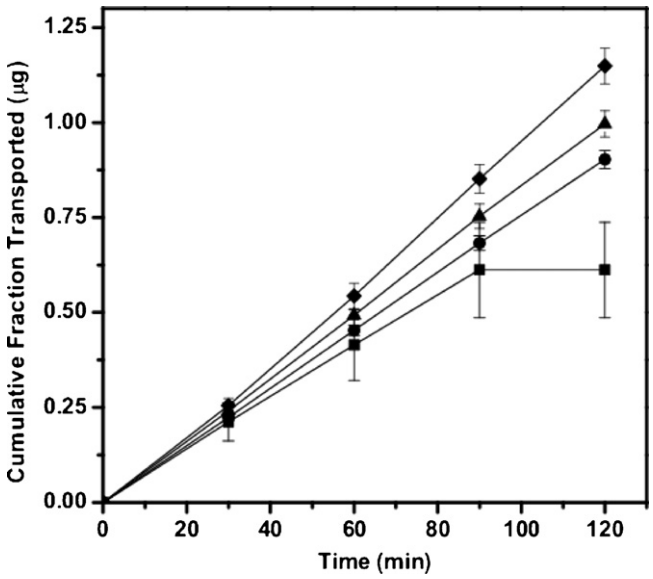

Fig. 7. Transport of EGCG through Caco-2 cell monolayers incubated with EGCG solution (■), or EGCG-loaded CS–CPP nanoparticle suspensions of different nanoparticle concentrations (●, 0.063 mg/mL; ▲, 0.125 mg/mL; □, 0.250 mg/mL) as a function of time with donor compartment pH set at pH 6.2.

The elevated permeation of EGCG after being encapsulated with CS–CPP nanoparticles could also be via the paracellular pathway. According to previous study, CS nanoparticles can adhere and infiltrate into the mucus layer covering on the surface of enterocyte, further to open the tight junctions of cell monolayers (Sung et al., 2008). Then, loading compounds released from CS nanoparticles can go via opened channel between enterocyte into systemic circulation rather than penetrate through the whole cell. Measurements of TEER of cell monolayers can be used to predict their paracellular permeability (Junginger, van der Merwe, Verhoef, Verheijden, & Kotze, 2004). As tight junctions open, the TEER of Caco-2 cell monolayers is significantly reduced by the passing of ions via their paracellular route. The decrease of TEER value of Caco-2 cell monolayers in present study can demonstrate the possible manner for EGCG's penetration through intestinal monolayers via paracellular pathway.

4. Conclusion

In present study, EGCG was encapsulated within homogeneously dispersed CS–CPP nanoparticles. AFM images showed that the nanoparticles were spherical in shape with particle size of 150 ± 4.3 nm and surface charge of 32.2 ± 3.3 mV. FTIR analysis results showed that cross-linking between the $-NH_3^+$ groups of CS with the $-P{=}O^-$ and $-COO^-$ groups of CPP, as well as the hydrogen bonding were the main interactions during the formation of CS–CPP nanoparticles. CS–CPP nanoparticles did not show any cellular toxicity to Caco-2 cell based on MTT assay. EGCG-loaded CS–CPP nanoparticles could enter Caco-2 cells in dose and time dependent manner, which was confirmed from the increased green fluorescence intensity inside the HepG2 cells with the increase of nanoparticle concentration and incubation time. Furthermore, the intestinal permeability and absorption of EGCG was enhanced obviously as delivered by CS–CPP nanoparticles. All of these results show that nanoparticles composed with polysaccharide and bioactive peptides of food origin are biocompatible and effective biomaterials for increasing the bioavailability of active small molecular weight polyphenols which are soluble but poorly absorbed.

Acknowledgments

This work was supported by a grant in-aid from United States Department of Agriculture National Research Initiative (2009-35603-05071, Q Huang), a grant in-aid from 863 Program, Ministry of Science and Technology, People's Republic of China (2007AA10Z351, X Zeng) and a Project Funded by the Priority Academic Program Development of Jiangsu Higher Education Institutions.

References

Acosta, E. (2009). Bioavailability of nanoparticles in nutrient and nutraceutical delivery. *Current Opinion in Colloid & Interface Science*, *14*(1), 3–15.
Amin, A. R. M. R., Kucuk, O., Khuri, F. R., & Shin, D. M. (2009). Perspectives for cancer prevention with natural compounds. *Journal of Clinical Oncology*, *27*(16), 2712–2725.
Artursson, P., Hubatsch, I., & Ragnarsson, E. G. E. (2007). Determination of drug permeability and prediction of drug absorption in Caco-2 monolayers. *Nature Protocols*, *2*(9), 2111–2119.
Barrand, M. A., Cooray, H. C., Janvilisri, T., van Veen, H. W., & Hladky, S. B. (2004). Interaction of the breast cancer resistance protein with plant polyphenols. *Biochemical and Biophysical Research Communications*, *317*(1), 269–275.
Cai, Y., Anavy, N. D., & Chow, H. H. S. (2002). Contribution of presystemic hepatic extraction to the low oral bioavailability of green tea catechins in rats. *Drug Metabolism and Disposition*, *30*(11), 1246–1249.
Chiu, Y. L., Ho, Y. C., Chen, Y. M., Peng, S. F., Ke, C. J., Chen, K. J., et al. (2010). The characteristics, cellular uptake and intracellular trafficking of nanoparticles made of hydrophobically-modified chitosan. *Journal of Controlled Release*, *146*(1), 152–159.
Frei, B., & Higdon, J. V. (2003a). Antioxidant activity of tea polyphenols in vivo: Evidence from animal studies. *The Journal of Nutrition*, *133*(10), 3275S–3284S.
Frei, B., & Higdon, J. V. (2003b). Tea catechins and polyphenols: Health effects, metabolism, and antioxidant functions. *Critical Reviews in Food Science and Nutrition*, *43*(1), 89–143.
Fu, S. K., Wu, Y., Yang, W. L., Wang, C. C., & Hu, J. H. (2005). Chitosan nanoparticles as a novel delivery system for ammonium glycyrrhizinate. *International Journal of Pharmaceutics*, *295*(1-2), 235–245.
Gaserod, O., Jolliffe, I. G., Hampson, F. C., Dettmar, P. W., & Skjak-Braek, G. (1998). The enhancement of the bioadhesive properties of calcium alginate gel beads by coating with chitosan. *International Journal of Pharmaceutics*, *175*(2), 237–246.
Hu, B., Wang, S. S., Li, J., Zeng, X. X., & Huang, Q. R. (2011). Assembly of bioactive peptide–chitosan nanocomplexes. *Journal of Physical Chemistry B*, *115*(23), 7515–7523.
Hu, B., Pan, C. L., Sun, Y., Hou, Z. Y., Ye, H., Hu, B., et al. (2008). Optimization of fabrication parameters to produce chitosan–tripolyphosphate nanoparticles for delivery of tea catechins. *Journal of Agricultural and Food Chemistry*, *56*(16), 7451–7458.
Hu, B., Wang, L., Zhou, B., Zhang, X., Sun, Y., Ye, H., et al. (2009). Efficient procedure for isolating methylated catechins from green tea and effective simultaneous analysis of ten catechins, three purine alkaloids, and gallic acid in tea by high-performance liquid chromatography with diode array detection. *Journal of Chromatography A*, *1216*(15), 3223–3231.
Hu, B., Ting, Y. W., Yang, X. Q., Tang, W. P., Zeng, X. X., & Huang, Q. R. (2012). Nanochemoprevention by encapsulation of (-)-epigallocatechin-3-gallate with bioactive peptides/chitosan nanoparticles for enhancement of its bioavailability. *Chemical Communications*, *48*, 2421–2423.
Huang, M., Khor, E., & Lim, L. Y. (2004). Uptake and cytotoxicity of chitosan molecules and nanoparticles: Effects of molecular weight and degree of deacetylation. *Pharmaceutical Research*, *21*(2), 344–353.
Huo, M. R., Zhang, Y., Zhou, J. P., Yu, D., & Wu, Y. P. (2009). Potential of amphiphilically modified low molecular weight chitosan as a novel carrier for hydrophobic anticancer drug: Synthesis, characterization, micellization and cytotoxicity evaluation. *Carbohydrate Polymers*, *77*(2), 231–238.
Junginger, H. E., van der Merwe, S. M., Verhoef, J. C., Verheijden, J. H. M., & Kotze, A. F. (2004). Trimethylated chitosan as polymeric absorption enhancer for improved peroral delivery of peptide drugs. *European Journal of Pharmaceutics and Biopharmaceutics*, *58*(2), 225–235.
Kaur, I. P., Kakkar, V., Singh, S., & Singla, D. (2011). Exploring solid lipid nanoparticles to enhance the oral bioavailability of curcumin. *Molecular Nutrition & Food Research*, *55*(3), 495–503.
Khan, N., Afaq, F., Saleem, M., Ahmad, N., & Mukhtar, H. (2006). Targeting multiple signaling pathways by green tea polyphenol (−)-epigallocatechin-3-gallate. *Cancer Research*, *66*(5), 2500–2505.
Kohane, D. S., Timko, B. P., & Dvir, T. (2010). Remotely triggerable drug delivery systems. *Advanced Materials*, *22*(44), 4925–4943.
Lambert, J. D., Hong, J., Yang, G. Y., Liao, J., & Yang, C. S. (2005). Inhibition of carcinogenesis by polyphenols: Evidence from laboratory investigations. *The American Journal of Clinical Nutrition*, *81*(1 Suppl.), 284S–291S.
Lambert, J. D., & Yang, C. S. (2003). Mechanisms of cancer prevention by tea constituents. *The Journal of Nutrition*, *133*(10), 3262S–3267S.

Please cite this article in press as: Hu, B., et al. Cellular uptake and cytotoxicity of chitosan–caseinophosphopeptides nanocomplexes loaded with epigallocatechin gallate. *Carbohydrate Polymers* (2012), doi:10.1016/j.carbpol.2012.03.015

Lvov, Y. M., Shutava, T. G., Balkundi, S. S., Vangala, P., Steffan, J. J., Bigelow, R. L., et al. (2009). Layer-by-layer-coated gelatin nanoparticles as a vehicle for delivery of natural polyphenols. *ACS NANO*, *3*(7), 1877–1885.

Manach, C., Scalbert, A., Morand, C., Remesy, C., & Jimenez, L. (2004). Polyphenols: Food sources and bioavailability. *The American Journal of Clinical Nutrition*, *79*(5), 727–747.

McClements, D. J., & Rao, J. (2011). Food-grade nanoemulsions: Formulation, fabrication, properties, performance, biological fate, and potential toxicity. *Critical Reviews in Food Science and Nutrition*, *51*(4), 285–330.

Minko, S., Motornov, M., Roiter, Y., & Tokarev, I. (2010). Stimuli-responsive nanoparticles, nanogels and capsules for integrated multifunctional intelligent systems. *Progress in Polymer Science*, *35*(1–2), 174–211.

Mukhtar, H., Siddiqui, I. A., Adhami, V. M., Bharali, D. J., Hafeez, B. B., Asim, M., et al. (2009). Introducing nanochemoprevention as a novel approach for cancer control: Proof of principle with green tea polyphenol epigallocatechin-3-gallate. *Cancer Research*, *69*(5), 1712–1716.

Nam, H. Y., Kwon, S. M., Chung, H., Lee, S. Y., Kwon, S. H., Jeon, H., et al. (2009). Cellular uptake mechanism and intracellular fate of hydrophobically modified glycol chitosan nanoparticles. *Journal of Controlled Release*, *135*(3), 259–267.

Panda, C. K., Manna, S., Mukherjee, S., Roy, A., & Das, S. (2009). Tea polyphenols can restrict benzo[*a*]pyrene-induced lung carcinogenesis by altered expression of p53-associated genes and H-ras, c-myc and cyclin D1. *Journal of Nutritional Biochemistry*, *20*(5), 337–349.

Sagalowicz, L., & Leser, M. E. (2010). Delivery systems for liquid food products. *Current Opinion in Colloid & Interface Science*, *15*(1–2), 61–72.

Sang, S., Lambert, J. D., Hong, J., Tian, S., Lee, M. J., Stark, R. E., et al. (2005). Synthesis and structure identification of thiol conjugates of (−)-epigallocatechin gallate and their urinary levels in mice. *Chemical Research in Toxicology*, *18*(11), 1762–1769.

Schmid, S. L., & Conner, S. D. (2003). Regulated portals of entry into the cell. *Nature*, *422*(6927), 37–44.

Shoichet, M. S. (2010). Polymer scaffolds for biomaterials applications. *Macromolecules*, *43*(2), 581–591.

Sugihara, N., Kadowaki, M., Tagashira, T., Terao, K., & Furuno, K. (2008). Presence or absence of a gallate moiety on catechins affects their cellular transport. *Journal of Pharmacy and Pharmacology*, *60*(9), 1189–1195.

Sung, H. W., Lin, Y. H., Sonaje, K., Lin, K. M., Juang, J. H., Mi, F. L., et al. (2008). Multi-ion-crosslinked nanoparticles with pH-responsive characteristics for oral delivery of protein drugs. *Journal of Controlled Release*, *132*(2), 141–149.

Tammela, P., Ekokoski, E., Garcia-Horsman, A., Talman, V., Finel, M., Tuominen, R., et al. (2004). Screening of natural compounds and their derivatives as potential protein kinase C inhibitors. *Drug Development Research*, *63*(2), 76–87.

Teitelbaum, D. H., Yang, H., & Finaly, R. (2003). Alteration in epithelial permeability and ion transport in a mouse model of total parenteral nutrition. *Critical Care Medicine*, *31*(4), 1118–1125.

Tsao, C. T., Chang, C. H., Lin, Y. Y., Wu, M. F., Wang, J. L., Han, J. L., et al. (2010). Antibacterial activity and biocompatibility of a chitosan-gamma-poly(glutamic acid) polyelectrolyte complex hydrogel. *Carbohydrate Research*, *345*(12), 1774–1780.

van Duynhoven, J., Vaughan, E. E., Jacobs, D. M., Kemperman, R. A., van Velzen, E. J., Gross, G., et al. (2011). Metabolic fate of polyphenols in the human superorganism. *Proceedings of the National Academy of Sciences of the United States of America*, *108*(Suppl. 1), 4531–4538.

Wood, E., Smith, J., & Dornish, M. (2004). Effect of chitosan on epithelial cell tight junctions. *Pharmaceutical Research*, *21*(1), 43–49.

Yang, C. S., Wang, X., Lu, G., & Picinich, S. C. (2009). Cancer prevention by tea: Animal studies, molecular mechanisms and human relevance. *Nature Reviews Cancer*, *9*(6), 429–439.

Yang, C. S., Maliakal, P., & Meng, X. (2002). Inhibition of carcinogenesis by tea. *Annual Review of Pharmacology and Toxicology*, *42*, 25–54.

Zhang, L., Zheng, Y., Chow, M. S. S., & Zuo, Z. (2004). Investigation of intestinal absorption and disposition of green tea catechins by Caco-2 monolayer model. *International Journal of Pharmaceutics*, *287*(1–2), 1–12.

Please cite this article in press as: Hu, B., et al. Cellular uptake and cytotoxicity of chitosan–caseinophosphopeptides nanocomplexes loaded with epigallocatechin gallate. *Carbohydrate Polymers* (2012), doi:10.1016/j.carbpol.2012.03.015